





Redundancy and Novelty Between ECG Leads Based on Linear Correlation

Utkars Jain¹, Adam A. Butchy¹, Michael T. Leasure¹, Veronica A. Covalesky^{2,3}, Daniel McCormick^{2,3} and Gary S. Mintz⁴

¹Heart Input Output Inc., 128 N. Craig Street, Suite 406, Pittsburgh, U.S.A.

²Cardiology Consultants of Philadelphia, Philadelphia, Pennsylvania, U.S.A.

³Jefferson University Hospital, Philadelphia, Pennsylvania, U.S.A.

⁴The Cardiovascular Research Foundation, New York, New York, U.S.A.

Keywords: Statistics, ECGs, Cardiac, Correlation.

Abstract: ECGs are a common diagnostic method for diagnosing cardiac pathologies. In this study, the Pearson correlation coefficient is used to examine the latent linear correlations between the leads of a standard 12-lead ECG. We utilize both the original ECG signals from the PTB-XL database and the reconstructed signal generated by a deep learning model, ECGio. We find that leads III, aVL, V1, and V2 are, on average, the leads with the most unique information due to their low correlation with other leads.

1 INTRODUCTION


Clinicians use a range of diagnostic techniques to detect and identify heart and circulatory problems. Electrocardiograms (ECGs), Troponin biomarker testing, coronary computed tomography angiograms (CCTAs), magnetic resonance imaging (MRI), positron emission tomography (PET), fractional flow reserve (FFR), and coronary angiography are the most frequently performed. These tests search for structural, vascular, or electrical abnormalities in the cardiovascular system of a patient (DeLaney et al., 2017). This paper focuses on the noninvasive, ubiquitous, and inexpensive electrocardiogram (ECG).


Invented in the 1870s, the ECG is a simple yet effective monitoring device for the heart's electrical beats and rhythms (AlGhatrif and Lindsay, 2012). The standard 12-lead ECG consists of nine electrodes connected to specified locations on the patient's body and one electrode serving as an electrical ground. The ECG machine then measures the voltage difference between specific electrodes on the body to generate waveforms that represent the building, release, and refractory phases of the heart's electrical cycle (Yang


et al., 2015). A bipolar electrode is created by subtracting voltage of the ground electrode from the voltage of another electrode. Unipolar have a single positive electrode and utilize a combination of the other electrodes to serve as the negative electrode (Derganc and Gomišček, 2021). ECGs can be configured in a variety of ways - all configurations differ based on the placement, location, and number of leads.

The 12-lead resting ECG is the most common (Harris, 2016) but several other types exist. Holter ECGs may contain 2, 3, 6, or even 12 leads and are used for continuous patient monitoring (DiMarco and Philbrick, 1990). There exist more complicated devices that use far more than 12 leads, and may even take a full-body reading with a vest-like device (Wang et al., 2019). Recent advancements in personal electronics have enabled the integration of 1-lead ECG devices into smartwatches (Samol et al., 2019). In table 1, we have a description of the 12 leads of the normal resting ECG system.

In this paper, we analyze the linear correlation between ECG leads as a measure of information redundancy using the standard 12-lead ECG and its associated leads. We determine if there are specific leads that carry less redundant information when compared to others. Prior research investigated the use of AI to more thoroughly analyze ECGs and how to use ECGs with fewer than 12 leads to improve ECG signals (Jain

^a <https://orcid.org/0000-0002-1800-0768>

^b <https://orcid.org/0000-0002-0096-0031>

^c <https://orcid.org/0000-0002-1488-712X>


^d <https://orcid.org/0000-0003-3296-8705>

Table 1: The 12 leads, the location of the positive and negative electrodes, and which heart surface they are thought to represent. “N” refers to neutral or electric ground. + Location refers to the positive electrode location, while - Location refers to the negative electrode location.

Lead	+ Location	- Location	Surface
I	Left Arm	Right Arm	Lateral
II	Left Leg	Right Arm	Inferior
III	Left Leg	Left Arm	Inferior
aVR	Right Arm	N	None
aVL	Left Arm	N	Lateral
aVF	Left Leg	N	Inferior
V1	Right side of sternum, 4th intercostal space	N	Septum
V2	Left side of sternum, 4th intercostal space	N	Septum
V3	Between V2 & V4	N	Anterior
V4	Left midclavicular line, 5th intercostal place	N	Anterior
V5	Left anterior axillary line	N	Lateral
V6	Left midaxillary line	N	Lateral

et al., 2022), we will use the methods of reconstruction to conclude if lead relationships are carried over. The correlation between distinct sets of leads will determine the redundancy and novelty of leads. Correlation will be defined by the Pearson correlation coefficient, also known as Pearson’s r.

2 RELATED WORKS

There have been other works that look into the calculation or use of inter-lead relationships or correlations between the lead of an ECG signals. Zhang et. al set out to investigate a possible reason as to why deep learning networks generalize pretty well in the detection of left bundle brach block (LBBB) even with small data sizes. They discovered that the correlation between lead V1 and other leads was close to 0, and a set correlation matrix can be indicative of LBBB (Zhang et al., 2022). Jekova et. al used inter-lead relationships in order to identify misplaced leads or cable reversals resulting in a flipped signal. They were able to build a robust algorithm that was able to identify cable reversals based on inter-lead relationships (Jekova et al., 2016).

3 METHODS

The Pearson correlation coefficient quantifies the linear correlation between two sets of data, providing a measure of how closely a linear model would fit to the data sets. An r value closer to 1 indicates a strong positive correlation while a value closer to -1 indi-

cates a strong negative correlation. An r value of 0 indicates no correlation between the two datasets. A generally accepted interpretation of the correlation is that if there is a strong positive or negative correlation that there is a redundancy in data (Schober et al., 2018). (I.e one dataset is a scaled version of the other.) If there is no correlation then there is novel information contained between the two different datasets. A visual example of the pearson correlation coefficient based on scatter plot data is seen in figure 1. A visual example using ECG data from patient file 06275 is shown in 2.

The Pearson correlation coefficient, or r is defined as:

$$r(y, \hat{y}) = \frac{\mathbb{E}[(y - \mu_y)(\hat{y} - \mu_{\hat{y}})]}{\sigma_y \sigma_{\hat{y}}} \tag{1}$$

Non-linear correlation cannot be measured by the Pearson correlation coefficient. This indicates that something may be highly uncorrelated in the linear sense but correlated in the nonlinear sense. To maintain a solid basis for interpretation, nonlinear correlations between leads fall outside the scope of this analysis.

We used 250 randomly selected patients from PTB-XL, a large public electrocardiography dataset, to conduct this study (Wagner et al., 2020). We chose 250 patients because this population served as the test set for our reconstruction experiments and will now serve as a good baseline to compare original signals and reconstructed signals. These were a random sample of healthy and pathological ECGs. One in which the original signal is present and one in which the signal has been reconstructed by a deep learning model called ECGio (Leasure et al., 2021). In a previous paper, the performance of ECGio in recreating ECGs using the same 250 patients was demonstrated (Jain et al., 2022). Maintaining patient consistency will prevent bias and preserve the same testing set. Since the deep learning model is expected to correct awry signals, we will determine whether these correlations are inherent to the ECGs or a result of noise.

The ECG signal input that was used to analyze correlation was standardized. Each ECG signal was clipped to represent 10 seconds of ECG time, with the form NxM, where M was the number of leads and N was the number of samples. Given that each signal lasted just 10 seconds, N was also equal to 10 times the sampling rate. We resampled the signal using Fast Fourier Transform (FFT) to reduce the sampling rate to 100Hz. This was done through the `scipy.signal.resample` method ¹ which assumes a periodic signal and transforms the signals to the fre-

¹docs.scipy.org/doc/scipy/reference/generated/scipy.signal.resample.html

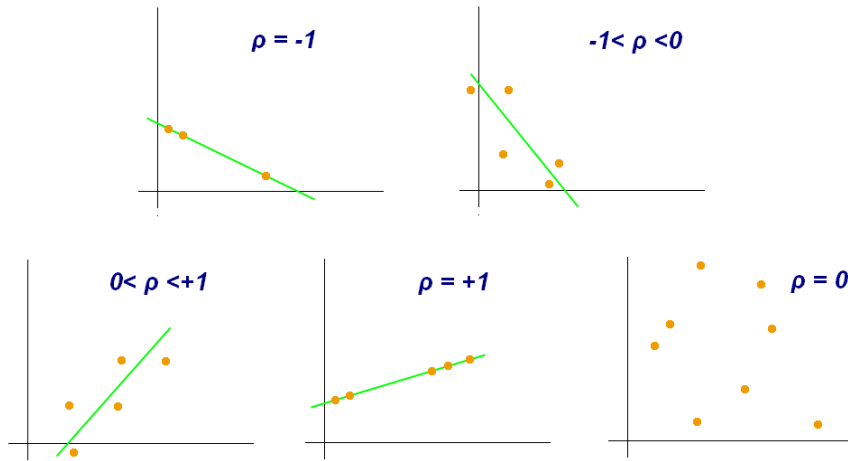


Figure 1: Visual example of the Pearson correlation coefficient based on scatter plot data. Illustration was provided by user Kiatdd from Wikimedia Commons, under the Creative Commons Attribution-Share Alike 3.0 Unported license.

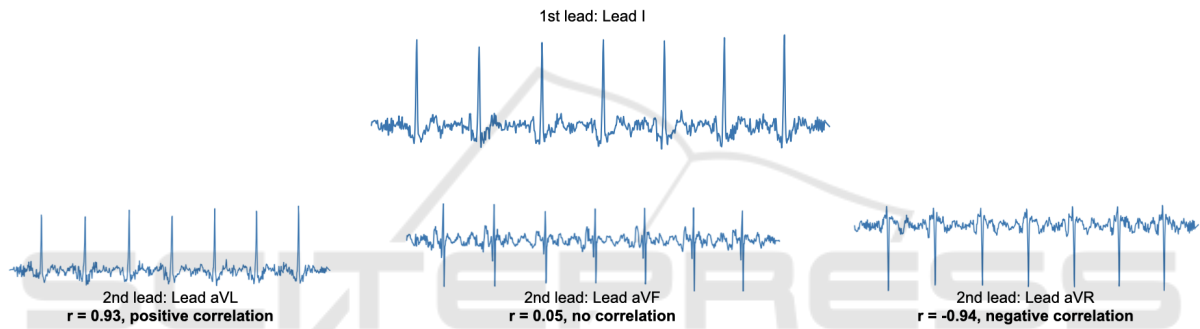


Figure 2: Visual example of the Pearson correlation coefficient based on ECG data. The initial comparative lead is lead I, and it is compared to the unipolar leads, lead I is shown to have a strong positive correlation to lead aVR, no correlation with lead aVF, and a strong negative correlation with lead aVL.

quency domain and removes unnecessary parts of the domain and transforms it back. We employed a Band-pass Butterworth filter with a passband beginning at 2Hz and ending at 40Hz to ensure that only information within this band of frequencies was kept while all others were discarded. Frequencies below 2Hz are where breathing and muscle noise may interfere with the signal (Li et al., 2017) and 40Hz is shown to be an adequate cutoff (Ricciardi et al., 2016).

The databased ECG signals were obtained with non-standardized minimum and maximum values in millivolts (mV). Conforming to best practices in machine learning (Jo, 2019), we scaled each ten-second ECG segment to values between [-1, +1] using equation 2, as is customary in deep learning to normalize input signals:

$$f(x) = 2 \frac{x - \min(x)}{\max(x) - \min(x)} - 1 \quad (2)$$

If x represented an ECG array in millivolts (mV), $\max(x)$ represented the largest value along x , and $\min(x)$ represented the minimum value along x . All

null values were transformed into zeros. Each signal was eventually detrended to the point where the isoelectric sections of the ECG were equal to zero.

The 12-lead standardized data served as the basis for calculating performance metrics. We did not employ raw voltage difference values as the reference to avoid a huge potential variance in the presence of muscle, movement, or electric noise creating signal-to-signal deviations. Mathematically, standardized signals would provide a more equitable comparison, whereas a direct comparison of performance indicators between our outcomes and those of others may not be prudent.

There are two primary methods to calculate the Pearson correlation coefficient. One is that we loop over every combination of the two leads in the ECG (e.g. lead I against itself, lead I against lead II, etc.) and apply the formula. This method would require us to go through every combination for every ECG. Meaning that in total there would be 66 calculations $\binom{12}{2} = \frac{12!}{2!(12-2)!}$ for a 12-lead ECG. This is not an insurmountable number of calculations, but in the case

for ECGs with many more leads, we would like a more scalable solution. The second method is a vectorized approach, i.e. creating a correlation matrix, in which there is a series of vector and matrix based calculations, resulting in many less overall calculations.

A correlation matrix was established for each of the 250 patients original and reconstructed ECGs. Each of these matrices were layered to generate a three dimensional tensor (size of 250x12x12). We did three alternative sets of operations of the first axis of this tensor: obtaining the mean, maximum, and minimum. After these processes were finished, there were 6 separate correlation matrices. A mean, maximum, and minimum correlation matrix for the original and reconstructed signals. The reason why maximum and minimum were selected was because we were under the assumption that there would high levels of correlations between any 2 leads for at least one patient - we were looking to determine whether there were any combinations in which their extremes broke the trend.

Algorithm 1: Algorithm for calculating correlation matrix.

Ensure: $X \rightarrow M \times N$ \triangleright X is the ECG matrix
 $X^* = X - \mu(X)$ \triangleright Subtract X by mean value in lead axis
 $X^{**} = X^* \cdot X^*$ \triangleright Matrix multiplication of X^*
 $Z = \sigma(\sqrt{\text{diag}(X^{**})})$ \triangleright Scaling based on covariance
 $R = \frac{X^{**}}{Z}$ \triangleright Correlation Matrix

4 RESULTS

The results of our two experiments are shown. In figures 3, 4, 5, 6, 7, and 8 we have heatmaps showing the cross correlation between all of the standard ECG leads for the original patient ECGs and the re-

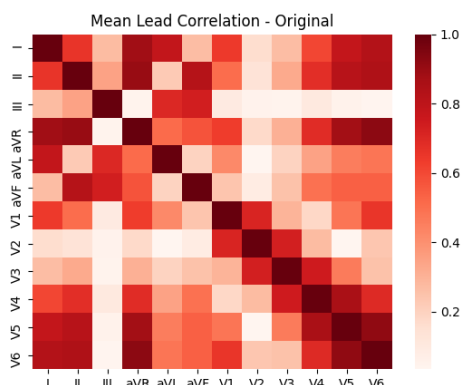


Figure 3: The figure below shows a heatmap of the mean correlation matrix over the population of patients examined with the original signals.

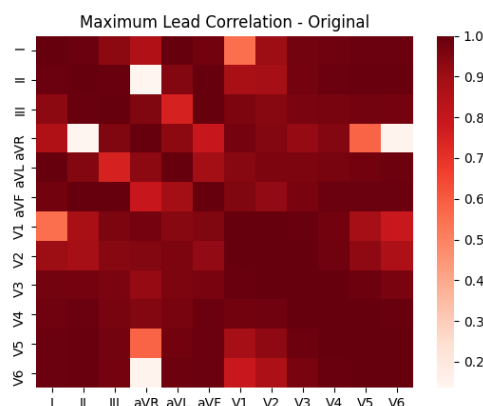


Figure 4: The figure below shows a heatmap of the maximum correlation matrix over the population of patients examined with the original signals.

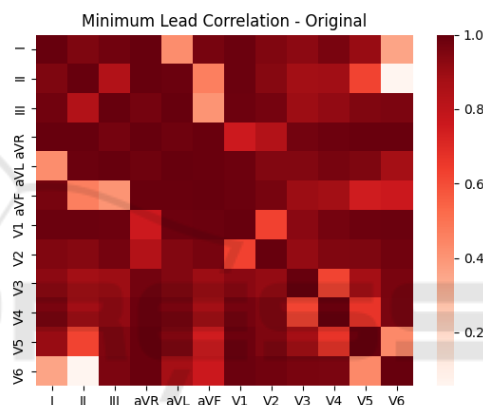


Figure 5: The figure below shows a heatmap of the minimum correlation matrix over the population of patients examined with the original signals.

constructed ones. Those that are more correlated have a darker color while the ones that are more uncorrelated are a lighter color. In tables 2 and 3 we see the mean, maximum, and minimum values for each lead when analyzing their correlations with other leads for the original ECGs and their reconstructions. In table 4 we examine the differences between the maximum and minimum correlation matrices for the original ECGs and their reconstructions.

5 DISCUSSION

The Pearson correlation coefficient is a prevalent approach for analyzing the linear relationship between continuous variables (Benesty et al., 2009). It can provide a great deal of broad information about variables with a single value. However, it should be highlighted that this is not a foolproof method for determining the correlation between signals or variables.

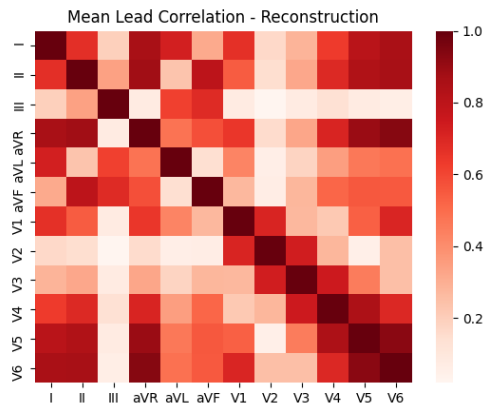


Figure 6: The figure below shows a heatmap of the mean correlation matrix over the population of patients examined with the reconstructed signals.

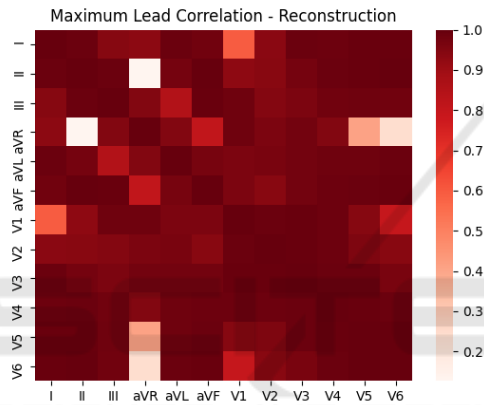


Figure 7: The figure above shows a heatmap of the maximum correlation matrix over the population of patients examined with the reconstructed signals.

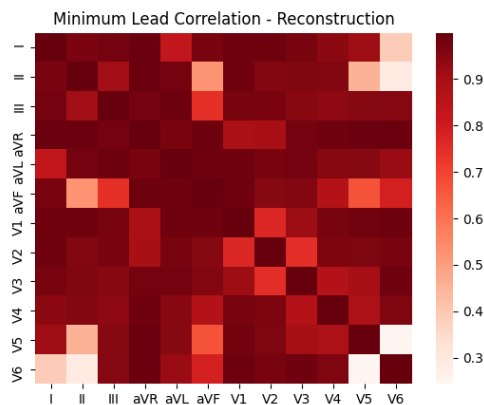


Figure 8: The figure above shows a heatmap of the minimum correlation matrix over the population of patients examined with the reconstructed signals.

We are simply evaluating the linear correlation of the signal. Essentially, we wish to determine whether the signals fluctuate synchronously. Do they rise or

Table 2: The table below shows the mean, maximum, and minimum correlations per lead when compared to other leads (sans the lead itself), when analyzing the mean correlation matrix from the 250 patients. Leads that shown to have significant degrees of uncorrelation are denoted with an *.

Lead	Mean r	Max r	Min r
I	0.205	0.832	-0.645
II	0.290	0.846	-0.507
III*	0.033	0.738	-0.272
aVR	-0.447	0.636	-0.903
aVL*	0.057	0.787	-0.516
aVF	0.233	0.828	-0.245
V1*	-0.128	0.714	-0.645
V2*	0.104	0.734	-0.163
V3	0.299	0.749	0.047
V4	0.359	0.862	-0.183
V5	0.319	0.920	-0.483
V6	0.254	0.920	-0.658

Table 3: The table below shows the mean, maximum, and minimum correlations per lead when compared to other leads (sans the lead itself), when analyzing the mean correlation matrix from reconstructions of the 250 patients. Leads that shown to have significant degrees of uncorrelation are denoted with an *.

Lead	Mean r	Max r	Min r
I	0.220	0.859	-0.863
II	0.291	0.867	-0.884
III*	0.050	0.687	-0.620
aVR	-0.450	0.649	-0.937
aVL*	0.065	0.732	-0.620
aVF	0.241	0.804	-0.579
V1*	-0.152	0.710	-0.707
V2*	0.102	0.739	-0.250
V3	0.299	0.749	-0.326
V4	0.362	0.850	-0.712
V5	0.318	0.930	-0.899
V6	0.256	0.930	-0.937

decrease simultaneously? All other connections are considered uncorrelated.

The Pearson correlation coefficient does not account for the magnitude of differences and is highly prone to outliers (Kim et al., 2015). For instance, there may be a large number of points centered about the origin and only a few along the x-axis. The Pearson correlation coefficient will depend heavily on how these few points behave. We attempted to preprocess and standardize the data in order to make fair comparisons, but this does not ensure the elimination of outliers.

In a typical 12-lead ECG setup there are 2-3 limb leads, leads attached to the arms or legs, and precordial (or chest) leads, leads attached to the chest.

Table 4: The table below shows the mean correlations per lead when compared to other leads (sans the lead itself), when analyzing the maximum and minimum correlation matrices from both the original 250 patients and the reconstructed ECGs.

Lead	Original Min	Original Max	Reconstructed Min	Reconstructed Max
I	-0.857	0.926	-0.904	0.940
II	-0.786	0.866	-0.816	0.901
III	-0.897	0.948	-0.940	0.961
aVR	-0.954	0.695	-0.969	0.710
aVL	-0.917	0.939	-0.957	0.964
aVF	-0.827	0.954	-0.859	0.964
V1	-0.929	0.903	-0.950	0.921
V2	-0.913	0.942	-0.924	0.960
V3	-0.895	0.974	-0.929	0.982
V4	-0.890	0.984	-0.937	0.985
V5	-0.828	0.939	-0.810	0.932
V6	-0.759	0.856	-0.773	0.855

The idea behind this setup is that limb leads provided information about the electrical propagation along a longer axis, while the chest leads provide information that is closer to the heart (Dower et al., 1990). These 2 sets of information combined can lead to a more holistic interpretation of the heart’s electrical activity. The unipolar leads (aVL, aVF, aVR) are constructed through a linear combination of the limb leads (Madias, 2008).

Lead III, which can occasionally be created from leads I and II (lead III = lead II - lead I), appears to be linearly uncorrelated with the mean of the original patients. This is unexpected because it can be viewed as a linear combination of leads I and II, yet there appears to be novel information in terms of correlation. Because lead I, II, and III are based upon a trigonometric relationship, it’s possible that correlations between them are not fully captured looking at linear relationships.

As seen in figures 3 and 6, the precordial leads, on average, seemed to be relatively uncorrelated when compared against the limb leads and the unipolar leads. This would be in line with the thought process that precordial leads are assessing different surfaces of the heart, and thus yield different information.

An intriguing phenomena in the maximum and minimum correlation of the original patients is that there are several correlations between leads that are close to +1 or -1. Even more unexpectedly, in our dataset, some correlations remained near 0 even when searching for the maximum or minimum value.

For instance, when searching for the maximal correlations, V6 has a correlation value of -0.14 when compared to aVR. This implies that, across the tested population, there was little correlation between these two leads, but V6 showed the strong correlation with other unipolar leads. aVR is a linear combination of

leads I and II, but its combination may contain information that differs significantly from what was previously believed (Williamson et al., 2006). Another similar case is between lead V6 and lead II, when looking for the minimum correlation case the value is -0.05. There may be an obvious explanation for unexpectedly significant correlations, namely that the lead was improperly positioned and hence captured signals that heavily overlapped with the domain of another lead for a particular ECG of a patient.

According to tables 2 and 3, leads III, aVL, V1, and V2 had the lowest average correlation. Using a threshold of 0.2, it was possible to determine which leads were uncorrelated. These leads offer information regarding the inferior, lateral, and septal surfaces of the heart (both lead V1, V2 offer information about the septal surface), which represent three of the heart’s four primary surfaces (lateral, inferior, septum, and anterior). Possible interpretation: these leads contain the most novel information regarding these surfaces. In the future, it may be necessary to determine if the novel information contained in these leads facilitates better levels of ECG reconstruction performance.

Our analysis uncovered the intriguing conclusion that the ECG reconstruction data closely resemble the original data. The goal of comparing the original correlation to that of the reconstruction was to determine if these correlations were intrinsic to the ECG itself and not the result of noise or lead placement, which the deep learning model is designed to correct.

Based on the similar levels of correlation, it may be concluded that a 12-lead ECG contains a latent structure that is known during model training. It is feasible that the model is just learning to match the output as closely as possible, without learning any intrinsic structure. In the future, it may be necessary to determine whether or not the model attempts to comprehend the ECG’s underlying structure when rebuilding the input.

6 CONCLUSION

In this study, we examined the average lead correlations of 250 patient ECG signals from the physionet PTB-XL database. We studied the original signals while they were being normalized and when they were being reconstructed using a novel deep learning technique. The mean, maximum, and minimum correlations between the leads of a 12-lead ECG were studied. Leads III, aVL, V1, and V2 were identified as the most uncorrelated in the ECG system.

REFERENCES

- AlGhatrif, M. and Lindsay, J. (2012). A brief review: history to understand fundamentals of electrocardiography. *Journal of community hospital internal medicine perspectives*, 2(1):14383.
- Benesty, J., Chen, J., Huang, Y., and Cohen, I. (2009). Pearson correlation coefficient. In *Noise reduction in speech processing*, pages 1–4. Springer.
- DeLaney, M. C., Neth, M., and Thomas, J. J. (2017). Chest pain triage: Current trends in the emergency departments in the united states. *Journal of Nuclear Cardiology*, 24(6):2004–2011.
- Derganc, J. and Gomišček, G. (2021). Teaching the basic principles of electrocardiography experimentally. *Advances in Physiology Education*, 45(1):5–9.
- DiMarco, J. P. and Philbrick, J. T. (1990). Use of ambulatory electrocardiographic (holter) monitoring. *Annals of internal medicine*, 113(1):53–68.
- Dower, G., Nazzal, S., Bullington, D., Pahlm, O., Haistey Jr, W., Marriott, H., and Bullington, R. (1990). Limb leads of the electrocardiogram: sequencing revisited. *Clinical cardiology*, 13(5):346–348.
- Harris, P. R. (2016). The normal electrocardiogram: Resting 12-lead and electrocardiogram monitoring in the hospital. *Critical Care Nursing Clinics*, 28(3):281–296.
- Jain, U., Butchy, A. A., Leasure, M., Covalesky, V. A., McCormick, D., and Mintz, G. H. (2022). 12-lead eeg reconstruction via combinatoric inclusion of fewer standard eeg leads with implications for lead information and significance. In *BIO SIGNALS*.
- Jekova, I., Krasteva, V., Leber, R., Schmid, R., Twerenbold, R., Müller, C., Reichlin, T., and Abächerli, R. (2016). Inter-lead correlation analysis for automated detection of cable reversals in 12/16-lead ECG. *Computer Methods and Programs in Biomedicine*, 134:31–41.
- Jo, J.-M. (2019). Effectiveness of normalization preprocessing of big data to the machine learning performance. *The Journal of the Korea institute of electronic communication sciences*, 14(3):547–552.
- Kim, Y., Kim, T.-H., and Ergün, T. (2015). The instability of the pearson correlation coefficient in the presence of coincidental outliers. *Finance Research Letters*, 13:243–257.
- Leasure, M., Jain, U., Butchy, A., Otten, J., Covalesky, V. A., McCormick, D., and Mintz, G. S. (2021). Deep learning algorithm predicts angiographic coronary artery disease in stable patients using only a standard 12-lead electrocardiogram. *Canadian Journal of Cardiology*.
- Li, J., Deng, G., Wei, W., Wang, H., and Ming, Z. (2017). Design of a real-time ECG filter for portable mobile medical systems. *IEEE Access*, 5:696–704.
- Madias, J. E. (2008). On recording the unipolar eeg limb leads via the wilson’s vs the goldberger’s terminals: avr, avl, and avf revisited. *Indian Pacing and Electrophysiology Journal*, 8(4):292.
- Ricciardi, D., Cavallari, I., Creta, A., Giovanni, G. D., Calabrese, V., Belardino, N. D., Mega, S., Colaiori, I., Ragni, L., Proscia, C., Nenna, A., and Sciascio, G. D. (2016). Impact of the high-frequency cutoff of band-pass filtering on ECG quality and clinical interpretation: A comparison between 40hz and 150hz cutoff in a surgical preoperative adult outpatient population. *Journal of Electrocardiology*, 49(5):691–695.
- Samol, A., Bischof, K., Luani, B., Pascut, D., Wiemer, M., and Kaese, S. (2019). Single-lead eeg recordings including einthoven and wilson leads by a smartwatch: a new era of patient directed early eeg differential diagnosis of cardiac diseases? *Sensors*, 19(20):4377.
- Schober, P., Boer, C., and Schwarte, L. A. (2018). Correlation coefficients: appropriate use and interpretation. *Anesthesia & Analgesia*, 126(5):1763–1768.
- Wagner, P., Strodthoff, N., Boussejot, R.-D., Samek, W., and Schaeffter, T. (2020). Ptb-xl, a large publicly available electrocardiography dataset.
- Wang, L.-H., Zhang, W., Guan, M.-H., Jiang, S.-Y., Fan, M.-H., Abu, P. A. R., Chen, C.-A., and Chen, S.-L. (2019). A low-power high-data-transmission multi-lead eeg acquisition sensor system. *Sensors*, 19(22):4996.
- Williamson, K., Mattu, A., Plautz, C. U., Binder, A., and Brady, W. J. (2006). Electrocardiographic applications of lead avr. *The American journal of emergency medicine*, 24(7):864–874.
- Yang, X.-L., Liu, G.-Z., Tong, Y.-H., Yan, H., Xu, Z., Chen, Q., Liu, X., Zhang, H.-H., Wang, H.-B., and Tan, S.-H. (2015). The history, hotspots, and trends of electrocardiogram. *Journal of geriatric cardiology: JGC*, 12(4):448.
- Zhang, C., Li, J., Pang, S., Xu, F., and Zhou, S. (2022). A 12-lead ECG correlation network model exploring the inter-lead relationships. *Europhysics Letters*, 140(3):31001.